Gas Processing Journal
Vol. 4, No. 2, 2016
http://gpj.ui.ac.ir

Improvement of Methanol Synthesis Process through a Novel Sorption-Enhanced Fluidized-bed Reactor,
Part I: Mathematical Modeling

M. Bayat
Department of Chemical Engineering, Faculty of Engineering, University of Bojnord, Bojnord, Iran

Article History
Received: 2017-04-03 Revised: 2017-10-12 Accepted: 2017-10-23

Abstract
In the first part of two section paper, a mathematical model of the fluidized bed reactor in the presence of in-situ water adsorbent for methanol synthesis is assessed. The bubbling two-phase regime is applied to model the fluidization concept. The binary adsorbent and catalyst particles system can be separated from each other based on their density difference. The heavy catalyst particles tend to sink and the light adsorbent particles tend to rise. The inducement for in situ water vapor removal by using adsorbent particles (Zeolite 4A) is to displace the water-gas shift equilibrium to improve methanol productivity. This is accomplished through the methanol synthesis process.

Simulation result indicate that selective adsorption of water in the fluidized bed configuration leads to 46.36% and 41.88% enhancement in methanol production and 26.143% and 25.63 % in selectivity, compared with the zero solid mass ratio condition and conventional reactor, respectively. This model is applied in a multi-objective optimization and decision making method to be presented in the upcoming study, Part II.

Keywords
Methanol synthesis; Mathematical model; Fluidized bed reactor; Zeolite 4A; Adsorption.

1. Introduction

Energy is a crucial constituent in human survival. Currently, a great volume of the energy is yield from non-renewable fossil fuel. The synthesis gas can commercially be converted into methanol through $CuO/ZnO/Al_2O_3$ catalyst. In general, a small improvement in main chemicals properties like in methanol would lead to significant energy conservation, environmental protection and thereupon profit increment (Schack et al., 1989). In order to improve the efficiency of industrial methanol synthesis reactor, several configurations are proposed (Rahimpour et al., 2010; Rahimpour and Elekaei, 2009; Rahimpour and Lotfinejad, 2008; Vakili et al., 2011).

In methanol production from synthesis gas, mainly three overall reactions are involved:

$$CO + 2H_2 \leftrightarrow CH_3OH \quad (1)$$

$$\Delta H_{298} = -90.55 kJ\,mol^{-1}$$

$$\Delta H_{298} = +41.12 kJ\,mol^{-1}$$
$$CO_2 + H_2 \leftrightarrow CO + H_2O \quad (2)$$

$$CO_2 + 3H_2 \leftrightarrow CH_3OH + H_2O$$
$$\Delta H_{298} = -49.43 kJ\,mol^{-1} \quad (3)$$

In this article, the reaction expression rates is from Graaf et al. (1990).

In the methanol reactor, only certain per-pass conversion of reactant is yield because of thermodynamic limitations. Hence, the reactant recycles loop and product separator are introduced to obtain a reasonable degree of reactant conversion. These methods are mostly expensive and cumbersome (Bayat et al., 2014b).

In methanol synthesis process, the sorption-enhanced process run through the fluidized bed reactor is found to be an appropriate

* Corresponding Author.
Authors' Email Address:
M. Bayat (m.bayat@ub.ac.ir),

ISSN (Online): 2345-4172, ISSN (Print): 2322-3251 © 2017 University of Isfahan. All rights reserved

method to overcome the thermodynamic limitation. Equilibrium can be shifted towards the formation of more products by selective adsorption of byproducts.

Johnsen et al. (2006) revealed that the contact of gas-solid in a bubbling fluidized bed lab scale reactor is enough to reach near equilibrium conditions. Almost 50 years ago, the suggestion of contacting gas and flowing particles inside a fluidized bed configuration was presented (Everett and Retallick, 1963).

Bayat et al. (Bayat et al., 2014a; Bayat et al., 2014b, c; Bayat et al., 2014d; Bayat et al., 2013, 2014e; Dehghani et al., 2014) have run studies on methanol synthesis and Fischer-Tropsch synthesis in the presence of water adsorbent particle. They have assessed the steady state packed bed reactor (Bayat et al., 2014a), membrane reactor (Bayat et al., 2014b), coupling reactor (Bayat et al., 2014e), unsteady state packed bed reactor (Dehghani et al., 2014) and dual bed reactor (Bayat et al., 2014c) for methanol synthesis process. Furthermore, Fischer–Tropsch synthesis process of gas flowing solid fixed bed configuration with in situ water adsorbent (Bayat et al., 2014d) and thermally coupled reactor (Bayat et al., 2013) are of concern. There exist a big volume of studies on sorption enhanced process (Bayat et al., 2014a; Bayat et al., 2014b, c; Bayat et al., 2014d; Bayat et al., 2013, 2014e; Dehghani et al., 2014) which prove the importance of how the utilization of zeolite 4A adsorbent is consumed in reversible reactions with water vapor formation, while, their results prove that the conversion of reactant is enhanced by removal of water from the reactor.

A mathematical model of fluidized bed reactor in the presence of regenerative water vapor adsorbent for methanol synthesis is presented in this article Part I. In Part II, uses this model is adopted to determine the optimal operating conditions for simultaneous maximization of methanol production and selectivity in SE-FMR.

2. Process Description

2.1. Conventional Methanol Reactor (CMR)

Methanol synthesis from syngas is run in a vertical non-isothermal heat exchanger reactor, where the tubes are packed by commercial $CuO/ZnO/Al_2O_3$ catalyst and surrounded by boiling water (Bayat et al., 2012).

2.2. Fluidized Bed Methanol Reactor (FMR)

The process in FMR configuration is similar to that of CMR with the exception of some changes: 1) in the inner tube side, fluidization is applied instead of the fixed catalyst bed through applying small catalyst size and 2) the feed synthesis gas enters the bottom of the reaction side to fluidize the catalyst bed. The parameters: tube diameter, length of reactor, feed operating condition are the same as that of the conventional reactor.

2.3. Sorption Enhanced-Fluidized-bed Methanol Synthesis Reactor (SE-FMR)

This configuration is almost similar to that of the FMR. The difference between them is attributed to consumption of zeolite 4A as water adsorbent. The chemical reactions over the fluidized catalyst begin and convert the feed synthesis gas into methanol along the sorption-enhanced reaction. In the next step, the adsorbent solid particles regenerate and fresh solids that enter the inlet of SE-FMR at every regeneration cycle. In this apparatus, the equilibrium is shifted toward the formation of more products by implementing the additional selective water adsorbent. In order to have a realistic assessment regarding industrial fixed-bed reactors, the same operating conditions of an actual industrial reactor are set. The inlet conditions of feed are extracted from study run by (Bayat et al., 2012). A conceptual schematic of sorption enhanced fluidized bed reactor is shown in Fig. 1.

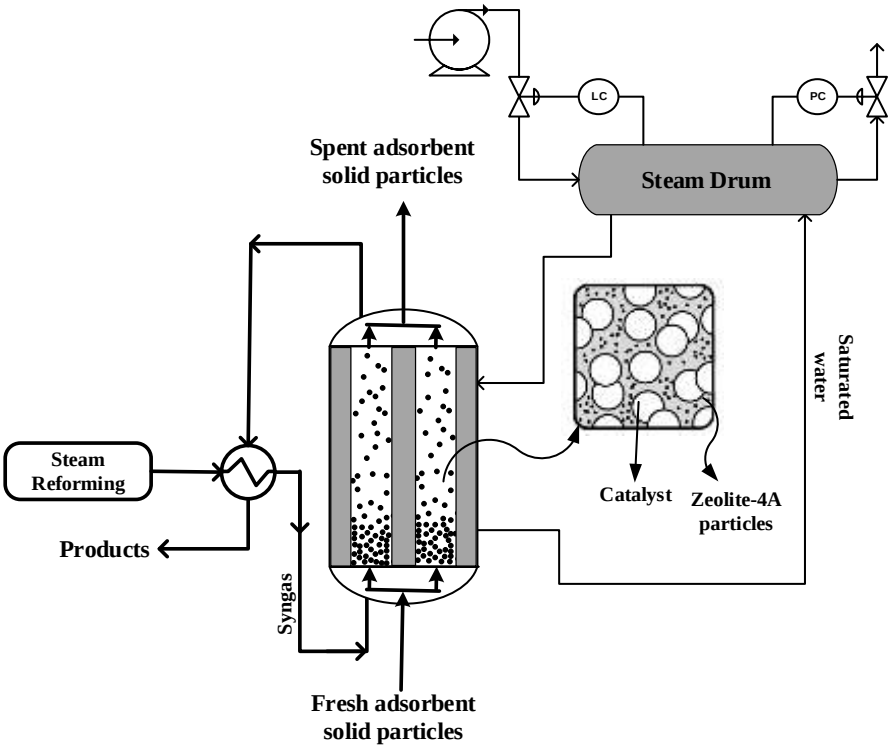

Figure. 1. A schematic Diagram of SE-FMR.

3. Mathematical Modeling

The following assumptions are considered in developing a mathematical model of SE-FMR:
(a) The equality between temperature of emulsion and bubble phase is assessed.
(b) Emulsion phase consist of adsorbent solids particle
(c) The constant average value of velocity for rising of bubbles is considered
(d) The Peng-Robinson EOS is assumed for PVT calculation
(e) The average size of spherical bubbles is assessed
(f) The temperature difference between catalyst phase and other phases is neglected
An element of length dz Fig. 2, is considered here. On the basis of the aforesaid assumptions, the equations of emulsion and bubble phase mass conservation are expressed as follows:

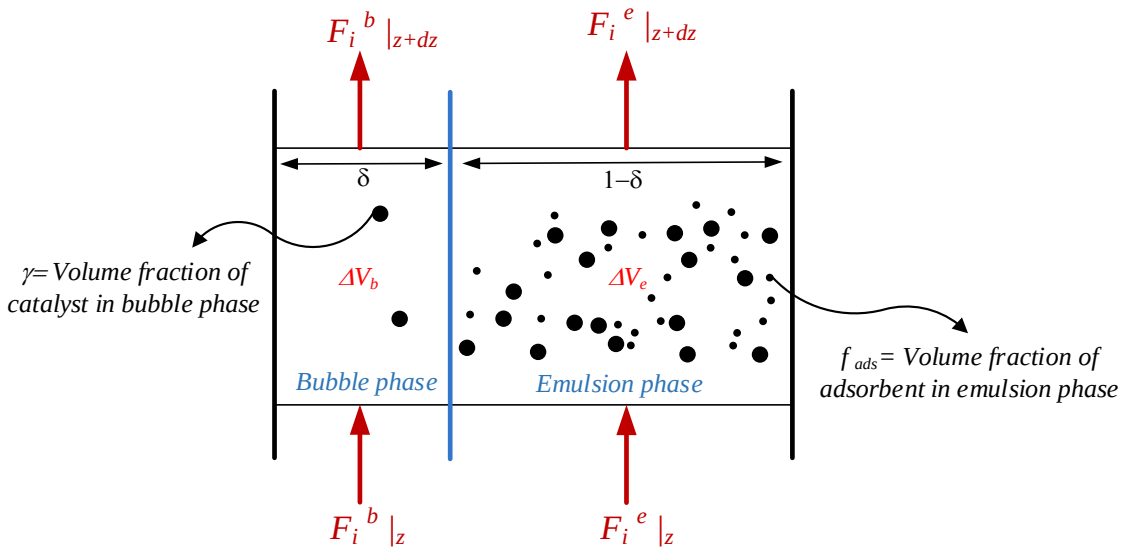

Figure. 2. Elemental Volume of SE-FMR.

3.1. Emulsion Phase:

$$-\frac{(1-\delta)}{A_c}\frac{dF_i^e}{dz}-K_{be,i}.a_b.c_t\left(y_i^e-y_i^b\right)+(1-\delta)\rho_e.\sum_{j=1}^{n}\nu_{ij}\left(-r_{ij}\right)$$
$$-\lambda k'_g\,\rho_{ads}\,f_{ads}(1-\delta)a'_s\,(q_e-q)=0$$
$$i=1,2,\ldots,N \qquad (4)$$

where, K_{bei} is the mass transfer coefficient between bubble phase and emulsion phase, y_i^e and y_i^b are the emulsion phase and bubble phase mole fraction, respectively. Parameter λ is assumed to be zero for the methanol, carbon dioxide, carbon monoxide, hydrogen, nitrogen and methane components and one for water component.

3.2. Bubble Phase:

$$-\frac{\delta}{A_c}\frac{dF_i^b}{dz}+K_{bei}c_t a_b(y_i^e-y_i^b)+\delta.\gamma.\rho_s.\sum_{j=1}^{3}\nu_{ij}\left(-r_{bij}\right)=0 \qquad (5)$$

where γ is the volume fraction of catalyst bed occupied by solid particles in bubble phase. The F_i^b and F_i^e are expressed as follows:

$$F_i^b=y_{ib}F^t \quad ,F_i^e=y_{ie}F^t \qquad (6)$$

The energy balance equation in emulsion and bubble phase is expressed as follow:

$$-\frac{1}{A_c}Cp_{Mix}\frac{d(F_tT_g)}{dz}+\frac{\pi D_L}{A_c}U_{Tube}(T_{shell}-T_g)-h'_f a'_s(T_g-T'_s)$$
$$(1-\delta)\rho_e.\sum_{j=1}^{3}r_{ej}(-\Delta H_{f,j})+\delta.\gamma.\rho_p.\sum_{j=1}^{3}r_{bj}(-\Delta H_{f,j})=0 \qquad (7)$$

3.3. Adsorbent Solid Phase

The mass balance of the adsorbent solid particle is calculated as follow:

$$u'_s\frac{dq}{dz}=k'_g a'_s(q_e-q) \qquad (8)$$

where, q is the water concentration in the solid particle adsorbent, and u'_s is the real velocity of zolite4A solids. The water adsorption/desorption isotherm on zeolite 4A particles is developed as Unilan equation presented by Zhu et al. (2005):

$$q_e=\frac{q_m}{2s}\ln\left(\frac{1+e^{s}KP_{H_2O}}{1+e^{-s}KP_{H_2O}}\right) \qquad (9)$$

The heterogeneity of the system is assessed based on parameter s. The parameter of water saturation capacity in solid particles is considered base on q_m. K parameter (adsorption affinity) and is calculated through van't Hoff equation as follow(Zhu et al., 2005):

$$K=K_0\exp\left[\frac{\overline{E}_{ads}}{RT_0}\left(\frac{T_0}{T}-1\right)\right] \qquad (10)$$

where, K_0 is the adsorption affinity at the reference temperature T_0 and $\overline{E}_{ads}$ is the average energy of adsorption. The parameter s has the following functional form of temperature dependence (Zhu et al., 2005).

$$s=s_0\frac{T_0}{T} \qquad (11)$$

The main parameters of this model are tabulated in Table 1 (Bayat et al., 2014a; Bayat et al., 2014b, c). For the solid phase adsorbent, one term for the heat transfer between the gas phase and solid adsorbent, and the other term state the released heat of adsorption (ΔH_{ads}) in energy balance equation:

$$u'_s\rho'_s Cp'_s\frac{dT'_s}{dz}=-\Delta H_{ads}S'\,a'_s(q_e-q)+h'_f a'_s(T_g-T'_s) \qquad (12)$$

3.4. Boundary Conditions

$y_i=y_{i0}$, $T_g=T_{g0}$, $q=0$ $\quad T_s'=T_{g0}$ $\quad at\ z=0$

Table 1. Main Parameter of Mathematical Modeling

Parameters	Value
Catalyst diameter (m), d_s	7.51×10^{-4}
Number of tubes (-)	2962
Length of reactor (m), L	7.022
Diameter of tube (m), D	38×10^{-3}
Catalyst density ($kg.m^{-3}$), ρ_p	2721
Adsorbent particle density ($kg.m^{-3}$), ρ'_S	1245
Flowing solids diameter (m), d'_s	3×10^{-4}
Specific heat of adsorption ($kJ.mol^{-1}$), ΔH_{ads}	64
Mass flux of water adsorption ($kg.m^{-2}.s^{-1}$), S'	0.1
Mass of catalyst in FBR (kg), (M_{cat})	2689.1
Mass of catalyst + Mass of adsorbent in SE-FR (kg)	2689.1
Thermal conductivity of solid wall ($Wm^{-1}K^{-1}$)	48
Saturation capacity (kmol/kg), q_m	15.81×10^{-3}
Adsorption affinity at reference temperature, K_0	4.722 kPa^{-1}
Average energy of adsorption, $\overline{E}_{ads}$	56.23 kJ/mol
Reference temperature, T_0 (K)	340.6 K
s_0	4.67

Here, the other useful correlations for heat transfer and physical properties are considered in solving the set of these developed models. The reported empirical correlations of the hydrodynamic parameters for SE-FMR in Table 2 are extracted from the study run by (Davidson and Harrison, 1963; Deshmukh et al., 2005; Goossens et al., 1971; Holman, 1989; Kunii and Levenspiel, 1991; Mori and Wen, 1975; Perry et al., 1977; Tatlıer and Erdem-Şenatalar, 2000). The mathematical modeling is explained in Appendix A.

Table 2. Properties of Physical Parameter, the Phenomenological Relationship for the Hydrodynamic Parameters, Heat and Mass Transfer Correlation

Parameter	Equation
Heat capacity of each component	$Cp_g = a + bT + cT^2 + dT^{-2}$
Heat capacity of mixture	$Cp_g = \sum y_i Cp_{gi}$
Heat capacity of adsorbent solids	$Cp'_s = \frac{4.2W + 0.0119T_s' - 3.0487}{1+W}$
Viscosity	$\mu = \frac{C_1 T^{C_2}}{1 + \frac{C_3}{T} + \frac{C_4}{T^2}}$
Archimedes number	$Ar = \frac{d_{p,Mix}^3 \rho_g (\rho_p - \rho_g) g}{\mu^2}$
Superficial velocity at minimum fluidization	$u_{mf} = \left(\frac{\mu}{d_{p,Mix}.\rho_g}\right)\left(\sqrt{739.84 + 0.0408.Ar} - 27.2\right)$
minimum fluidization bed voidage	$\varepsilon_{mf} = 0.586.Ar^{-0.029}\left(\rho_g / \rho_p\right)^{0.021}$
Mixture density and diameter	$\frac{1}{\rho_{Mix}} = \frac{w_c}{\rho_{cat}} + \frac{w_s}{\rho_s}$ $\frac{1}{\rho_{Mix}.d_{p,Mix}} = \frac{w_c}{\rho_{cat}.d_{p,cat}} + \frac{w_s}{\rho_s.d_s}$
Bubble diameter	$d_{bo} = 0.365(u_o - u_{mf})^2$ $d_{bm} = 0.00853\left(1 + 0.272\left(u_0 - u_{mf}\right)\right)^{1/3}.\left(1 + 0.0684z\right)^{1.21}$ $d_{b,avg} = d_{bm} - (d_{bm} - d_{bo})\exp(-0.3z/D)$
Mass transfer coefficient (bubble-emulsion phase)	$K_{be} = \frac{u_{mf}}{3} + [(4D_{jm}\varepsilon_{mf}u_b / \pi d_b)]^{1/2}$
Bubble rising velocity	$u_{b,avg} = u - u_{mf} + 0.711\sqrt{gd_b}$
Volume fraction of bubble phase to overall bed	$\delta = (u - u_{mf})/u_b$
Specific surface area for bubble	$a_b = 6\delta / d_b$
Density for emulsion phase	$\rho_e = \rho_P(1 - \varepsilon_{mf})$
Solid velocity	$u'_s = \alpha\delta u_b / (1 - \delta - \delta\alpha)$
Fluidized bed heat transfer coefficient	$Nu = \frac{h_i D_i}{k} = 420\left(\frac{\rho_s}{\rho_g}\mathrm{Re}_t\right)^{0.3}\left(\frac{\mu_g}{g\rho_s^2 d_{p,Mix}^3}\right)^{0.3}(pr)^{0.3}$
Heat transfer coefficient of boiling water in the shell side	$h_o = 7.96(T - T_{sat})^3\left(\frac{P}{P_a}\right)^{0.4}$
Overall heat transfer coefficient	$\frac{1}{U_i} = \frac{1}{h_i} + \frac{A_i\, ln(D_o/D_i)}{2\pi LK_w} + \frac{A_i}{A_o}\frac{1}{h_o}$

3.5. Peng-Robinson Equation of State

The well-known equation in thermodynamics is Peng and Robinson (1976), that is, the equation of state (EOS), formulated as:

$$P = \frac{RT}{v-b} - \frac{a}{v(v+b)+b(v-b)} \quad (13)$$

The compressibility factor for both phases (liquid and vapor phases) is developed as follows:

$$Z^3 + (B-1)Z^2 + (A-2B-3B^2)Z + (B^2+B^3-AB) = 0 \quad (14)$$

where,

$$A = \frac{aP}{(RT)^2} \quad (15)$$

$$B = \frac{bP}{(RT)} \quad (16)$$

For multi-component when the gas phase contains methane, carbon dioxide and nitrogen, the phase equilibrium is calculated as:

$$k_{ij} = \delta_2 T_{rj}^2 + \delta_1 T_{rj} + \delta_0 \quad (17)$$

4. Numerical Solution

The mathematical model consists of the mass and energy balance equation in bubble, emulsion and adsorbent phase, rate expression of the kinetic model, transport property and other supplementary correlation. This set of Differential-Algebraic Equations (DAE's) is solved through the Gear's method (ode15s) in MATLAB programming environment.

5. Model Validation

Wagialla and Elnashaie (1991) simulated the methanol synthesis process in a fluidized-bed reactor at steady state based on bubbling regime. This validated data is applied in comparing with the simulation results of SE-FMR. As it observed in Table 3, the results of simulation data are in perfect agreement with the Wagialla's data.

Table 3. Comparison between Simulation and Wagialla's Model

Component	Wagialla's model	Fluidized bed reactor model	Deviation (%)
Carbon monoxide	0.01881	0.0179	-4.84
Hydrogen	0.73512	0.7538	2.54
Methanol	0.04744	0.0492	3.71
Carbon dioxide	0.02838	0.0312	9.93
Water	0.01809	0.0168	-7.131
Nitrogen	0.02356	0.0231	-1.95
Methane	0.1286	0.1121	-12.8

6. Results and Analysis

The following definition is introduced to assess the mass ratio:

$$M_{ratio} = \frac{Mass\ of\ Adsorbnet\ Solid}{Mass\ of\ Catalyst} \quad (18)$$

In this part, steady-state simulation of SE-FMR is assessed for the base case of mass fraction ratio (M_{ratio}), which is 0.2.

6.3. Simulation Results

The temperature profiles of reacting gas in the axial direction of CMR, FMR and SE-FMR are shown in Fig. 3. The thermal equilibrium can be worse at high temperature in exothermic methanol synthesis process. The risk of catalyst deactivation through coking and sintering is diminished at minor temperatures, hence, the control of temperature in the fluidized bed reactors is easier than that of fixed beds. In excellent heat transfer, fluidized beds dominate the limitations of packed-bed methanol reactors; the temperature profile does not rise suddenly at first 2 m of the reactor. In the methanol synthesis process, the upper limit temperature for the $CuO/ZnO/Al_2O_3$ catalyst must be kept at about 543 K to avoid deactivation. Gas phase temperature profile of SE-FMR is higher than FMR, and this is due to H_2O adsorption as zeolite 4A adsorbent that boosts the reaction rate, thus discharging more heat in the interior of SE-FMR.

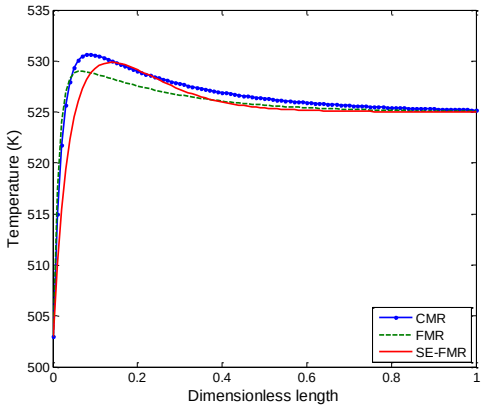

Figure. 3. Gas Phase Temperature in Axial Direction of CMR, FMR and SE-FMR

The carbon dioxide, carbon monoxide, hydrogen and water molar flow rate of SE-FMR, FMR and CR are shown in Figs. 4 (a)-(d). As observed in Fig. 4(a), the molar flow rate of CO_2 in this new configuration is lower than the other ones. The WGS reaction at reverse direction becomes faster with the removal of in-situ H_2O. Consequently, CO_2 and H_2 consumption rate are improved, Figs. 4 (a) and (d)) and CO production rate is increased along the SE-FMR rather than the CMR and even FMR (Fig. 4 (b)). As illustrated in Fig. 4 (c), the water production as well as catalyst recrystallization of this new configuration decreases duo to adsorption of water by adsorbent solid particles.

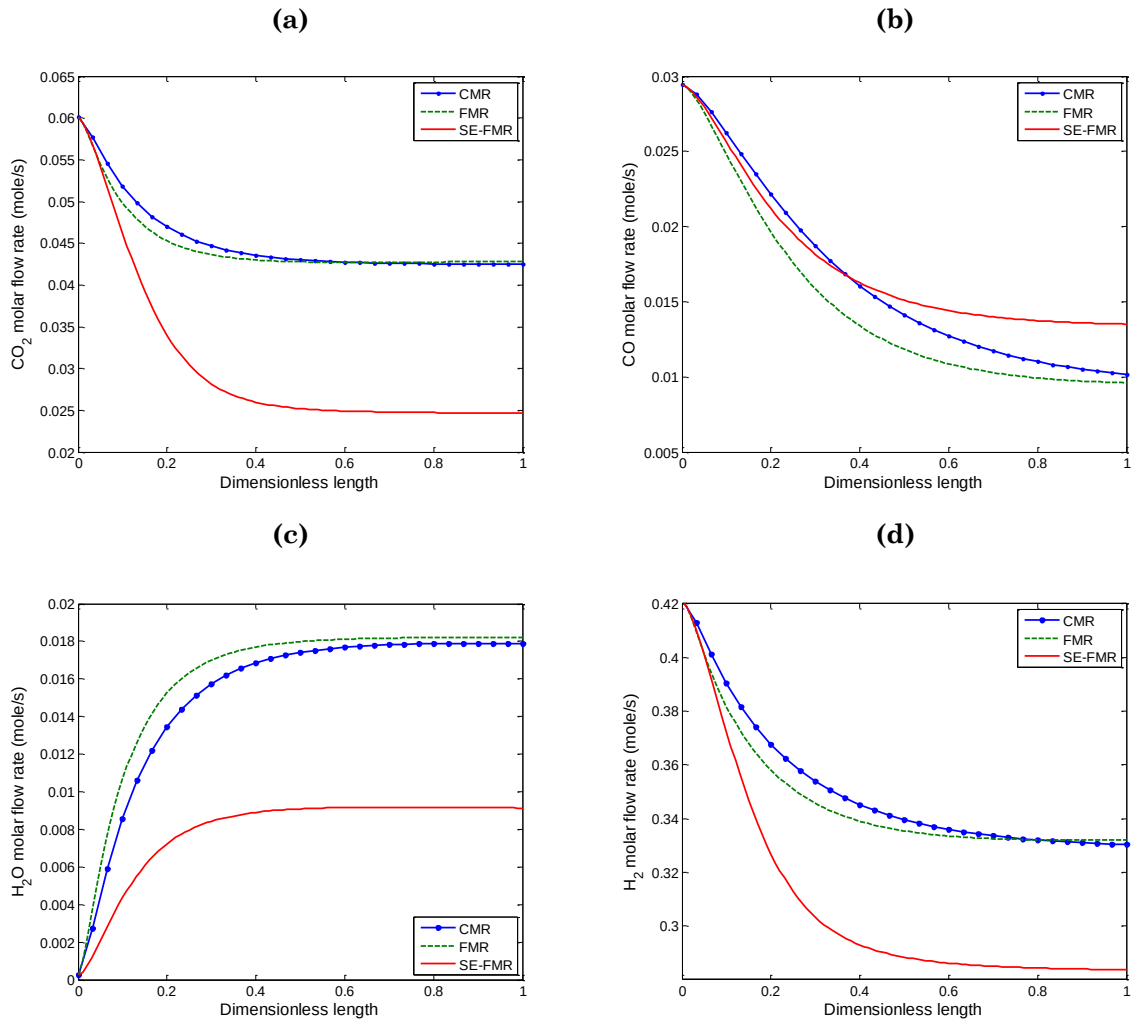

Figure. 4. Molar Flow Rate of (a) Carbon Dioxide, (b) Carbon Monoxide, (c) Water and (d) Hydrogen in Axial Direction of Three Different Configurations

The methanol production rate and selectivity of CR, FMR and SE-FMR are shown in Fig. 5 (a) and (b). The predicted SE-FMR reveal that the selectivity and methanol production rate is noticeably higher than the without adsorption. The idealistic effect of consuming zeolite 4A adsorbents in the SE-FMR enhances the reaction of CO_2 hydrogenation toward methanol production.

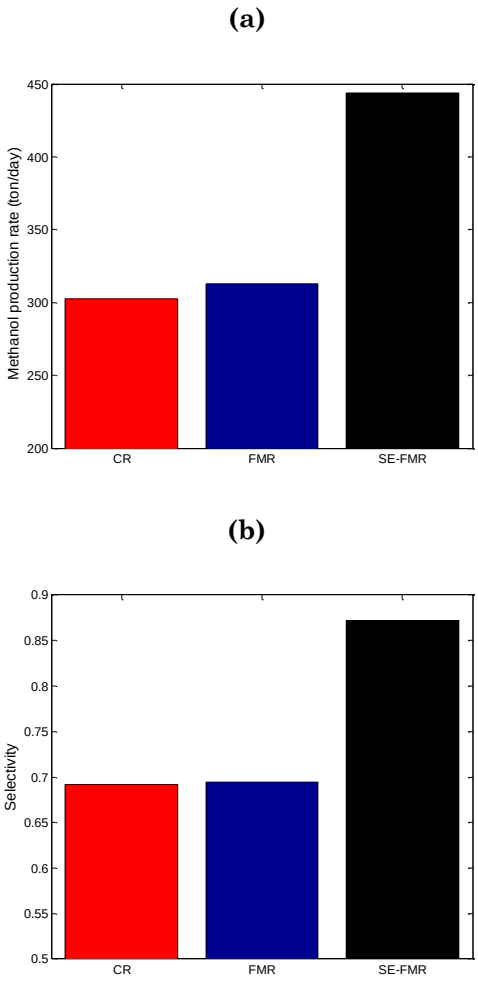

Figure. 5. Profiles of (a) Methanol Production Rate and (b) Selectivity in CMR, FMR and SE-FMR.

6.4. Influence of the Adsorbent/ Catalyst Mass Ratio

The methanol production rate and selectivity profile at different bed compositions is illustrated in Fig. 6 (a) and (b), where, although adding adsorbent to the reactor influence the weigh factor in enhancing the methanol production rate and selectivity, but it can have an adverse effect on the reactor length required for the complete methanol synthesis. It is observed that there exists a bed composition beyond which the methanol synthesis cannot be accomplished. Here it is evident that the composition of the bed should be well controlled, therefore, in part II, the mass fraction of adsorbent is selected as the decision variable.

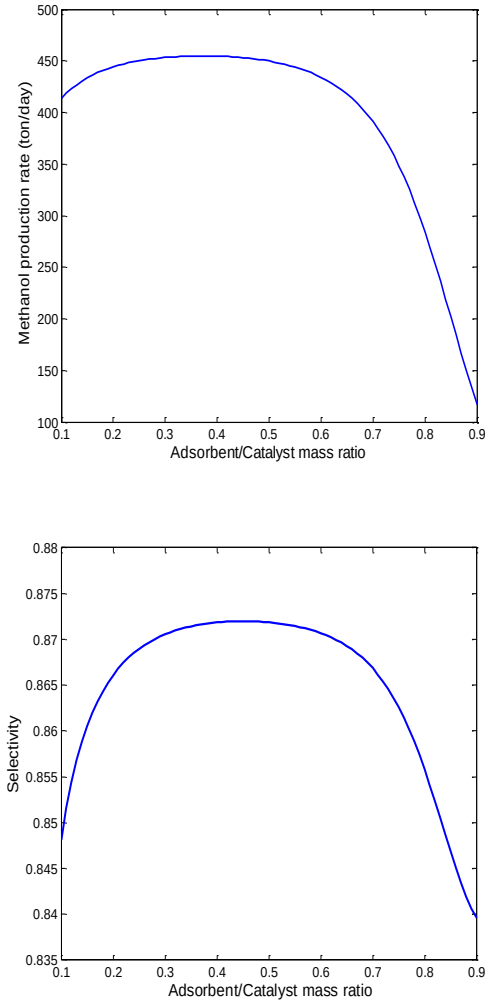

Figure. 6. Influence of the Adsorbent/ Catalyst Mass Ratio on (a) Methanol Production Rate and (b) Selectivity of SE-FMR

6.5. Influence of the Adsorbent Solid Diameter

The variation of adsorbent solid diameter over SE-FMR performance is studied in Fig. (7). In Figs. 7 (a) and (b) exhibit the effect of adsorbent solid diameter on reaction rate at the reactor exit. By increasing the adsorbent solid diameter, the amount of reaction rate increases per unit catalyst volume, and then decrease Fig 7 (a) and (b). Hydrogenation of carbon monoxide (r_1) and dioxide (r_3) are two

factors influencing the methanol concentration. According to Eqs. (1) and (3) here the overall methanol reaction rate is equal to methanol formation through the CO hydrogenation (r_1) plus methanol formation through CO_2 hydrogenation (r_3). The adsorbent solid diameter versus overall reaction rate of methanol is shown in Fig (7) (c). An increase in the adsorbent solid diameter from 0.1 to 1.1 mm increases the net of methanol formation reaction and then decreases. Hence, the overall reaction rate of methanol is maximized when the adsorbent solid diameter is 0.22 mm. The influence of adsorbent solid diameter on the methanol production rate is shown in Fig. 7 (c).

The trend of the overall reaction rate and production rate of methanol profiles are comparable. The overall maximum reaction rate and the methanol production rate are located at the same adsorbent solid diameter, 0.22 mm.

The effect of adsorbent solid diameter on selectivity at the outlet section of reactor is shown in Fig. 7 (d). In Fig. 7 (c) and (d) follow the same trend. An increase in the adsorbent solid diameter from 0.1 to 1.1, cause a sharp increase in selectivity up to 0.8762 and maximize the selectivity of methanol and then decreases smoothly to 0.8729, Fig. (7) (d).

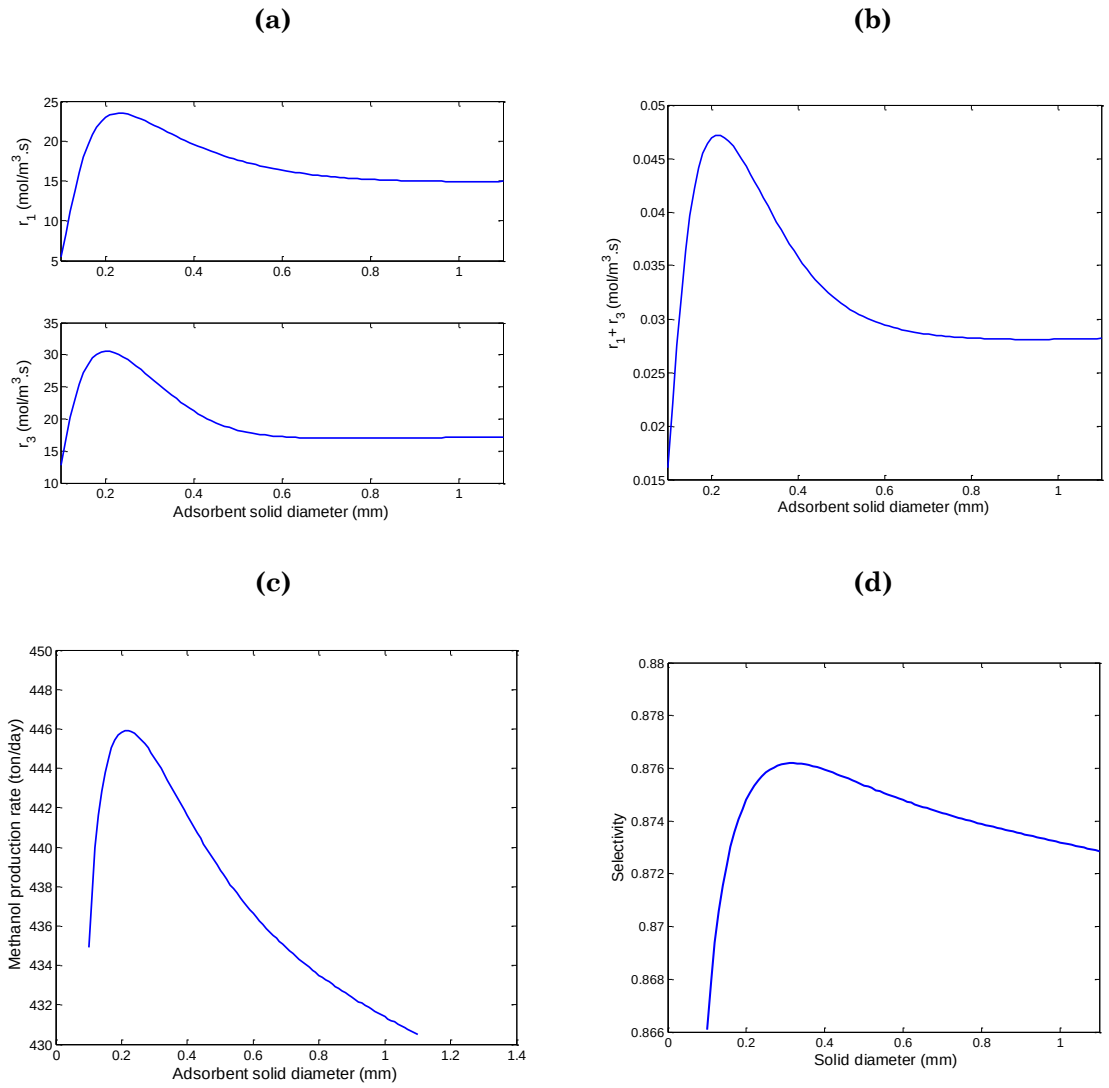

Figure. 7. Influence of the Adsorbent Solid Diameter on (a) Reaction Rate of CO and CO_2 Hydrogenation, (b) Summation Reaction Rate of them, (c) Methanol Production Rate and (d) Selectivity of SE-FMR

7. Conclusion

The methanol synthesis process is exothermic and restricted due to the thermal equilibrium. The fixed bed methanol reactor has disadvantages like low effectiveness factors coefficient and low heat transfer. Hence, one of the best manners to remove this disadvantage is applying a sorption enhanced fluidized-bed reactor, with an inherently low pressure drop through the catalytic bed. A steady state two phase theory of bubbling regime is developed for the simulation of (SE-FMR). The simulation results indicate that there is favorable profile of temperature in reaction side with 46.36% and 41.88% enhancement in the methanol productivity in comparison with FMR and CMR, respectively. Enhancements of 26.143% and 25.63% in the selectivity relative to the other configuration are observed as well. Finally, the effects of adsorbent on catalyst mass ratio and adsorbent solid diameter on the methanol production rate are obtained.

In the companion contribution (Part II), the mathematical model is integrated into the optimization procedure using NSGA-II algorithm and decision making method, in order to optimize key operating condition of SE-FMR.

Appendix A. Developing the Governing Equations

A differential element as shown in Fig. 2 is considered along the axial direction where the corresponding equations of mass and energy balance are developed.

A.1. Mass Balance:

A.1.1. Emulsion phase:

$$\begin{pmatrix}\text{Molar flow rate}\\ \text{of } i \text{ assuming the}\\ \text{entire bed is filled}\\ \text{with emulsion}\end{pmatrix}\times\begin{pmatrix}\text{Fraction of the}\\ \text{bed occupied}\\ \text{by emulsion}\end{pmatrix}=\left(F_i^e\right)(1-\delta) \tag{A-1}$$

$$\begin{pmatrix}\text{Moles}\\ \text{in}\end{pmatrix}-\begin{pmatrix}\text{Moles}\\ \text{out}\end{pmatrix}-\begin{pmatrix}\text{Moles transported}\\ \text{to bubble surface}\end{pmatrix}+\begin{pmatrix}\text{Moles reacted in}\\ \text{emulsion phase}\end{pmatrix}-\begin{pmatrix}\text{Moles transported to}\\ \text{adsorbent solid surface}\end{pmatrix}=0 \tag{A-2}$$

$$\begin{pmatrix}\text{Moles}\\ \text{in}\end{pmatrix}-\begin{pmatrix}\text{Moles}\\ \text{out}\end{pmatrix}\left(=F_i^e\big|_z-F_i^e\big|_{z+dz}\right)\times(1-\delta) \tag{A-3}$$

$$\begin{pmatrix}\text{Moles transported}\\ \text{to bubble surface}\end{pmatrix}=k_{be,i}\left(\frac{m}{s}\right).\Delta S_b\left(m^2\right).c_t\left(\frac{mole}{m^3}\right)\left(y_i^e-y_i^b\right) \tag{A-4}$$

$$\begin{pmatrix}\text{Moles reacted in}\\ \text{catalytic reaction}\end{pmatrix}=\Delta V_e\left(m^3\ emulsion\right)\times\rho_s\left(\frac{kg\,cat}{m^3 cat}\right)\times\left(1-\varepsilon_{mf}\right)\left(\frac{m^3 cat}{m^3\ emulsion}\right).\sum_{m=1}^{n}\nu_{ij}\left(-r_{ij}\right)\left(\frac{mole}{kg\,cat.s}\right) \tag{A-5}$$

$$\begin{pmatrix}\text{Moles transported to}\\ \text{adsorbent solid surface}\end{pmatrix}=k'_g\left(\frac{m}{s}\right)\times\Delta S_s\left(m^2\right)\times(q_e-q)\left(\frac{mole}{kg\ of\ adsorbent}\right)\times\rho_{ads}\left(\frac{kg\ of\ adsorbent}{m^3\ ads}\right)\times f_{ads}\left(\frac{m^3\ ads}{m^3\ emulsion}\right)(1-\delta)\left(\frac{m^3\ emulsion}{m^3}\right)\begin{cases}0 & i\neq H_2O\\ 1 & i=H_2O\end{cases} \tag{A-6}$$

here, k'_g is the gas–sorbent mass transfer coefficient (m/s), ρ_{ads} is the adsorbent density (kg of ads/m^3 ads), f_{ads} is the volume fraction of adsorbent in emulsion phase (m^3 ads /m^3 emulsion), δ is the volume fraction of bubble phase rather than total bed volume (m^3 bubble

/m³), q is the concentration of water in the adsorbent solids (mol/kg of adsorbent), q_e is the equilibrium concentration of water on the adsorbent (mol/kg of adsorbent), ΔS_b and ΔS_s are the external bubble and adsorbent solid surface area, respectively, contained in the volume element. The steady-state mole balance then converts into:

$$\left(F_i^e\Big|_z - F_i^e\Big|_{z+dz}\right)\times(1-\delta) - k_{be,i}\Delta S_b.c_t\left(y_i^e - y_i^b\right) + \Delta V_e \times \rho_e.\sum_{m=1}^{n}\nu_{ij}\left(-r_{ij}^e\right)$$
$$-k'_g\times\Delta S_s\times(q_e-q)\times\rho_{ads}\times f_{ads}(1-\delta)\times\begin{cases}0 & i\neq H_2O\\ 1 & i=H_2O\end{cases}=0 \qquad \text{(A-7)}$$

Dividing through by $\Delta V_t = A_c.\Delta z$ yields:

$$(1-\delta)\left(\frac{F_i^e\Big|_z - F_i^e\Big|_{z+dz}}{A_c\Delta z}\right) - k_{be,i}\frac{\Delta S_b}{\Delta V_t}.c_t\left(y_i^e - y_i^b\right) + \frac{\Delta V_e}{\Delta V_t}\times\rho_e.\sum_{m=1}^{n}\nu_{ij}\left(-r_{ij}\right)$$
$$-k'_g\times\frac{\Delta S_s}{\Delta V_t}\times(q_e-q)\times\rho_{ads}\times f_{ads}(1-\delta)\times\begin{cases}0 & i\neq H_2O\\ 1 & i=H_2O\end{cases}=0 \qquad \text{(A-8)}$$

The effective area for mass transfer, a_b and a'_s, is the bubble and adsorbent particle surface area per unit bed volume, respectively:

$$a_b = \frac{\Delta S_b}{\Delta V} \qquad \text{(A-9)}$$

$$a'_s = \frac{\Delta S_s}{\Delta V} \qquad \text{(A-10)}$$

where, $\frac{\Delta V_e}{\Delta V_t} = (1-\delta)$ is the emulsion phase volume as a fraction of total bed volume (m³ emulsion /m³).

As the volume element becomes small, it approaches the differential volume element and the final mole balance equation becomes:

$$-\frac{(1-\delta)}{A_c}\frac{dF_i^e}{dz} - k_{be,i}.a_b.c_t\left(y_i^e - y_i^b\right) + (1-\delta)\times\rho_e.\sum_{m=1}^{n}\nu_{ij}\left(-r_{ij}\right)$$
$$-k'_g\times a'_s\times(q_e-q)\times\rho_{ads}\times f_{ads}(1-\delta)\times\begin{cases}0 & i\neq H_2O\\ 1 & i=H_2O\end{cases}=0 \qquad \text{(A-11)}$$

Eq. (A-11) can be rewritten as:

$$-\frac{(1-\delta)}{A_c}\frac{dF_i^e}{dz} - k_{be,i}.a_b.c_t\left(y_i^e - y_i^b\right) + (1-\delta)\times\rho_e.\sum_{m=1}^{n}\nu_{ij}\left(-r_{ij}\right)$$
$$-\lambda k'_g\times\rho_{ads}\times f_{ads}(1-\delta)\times a'_s\times(q_e-q)=0 \qquad \text{(A-12)}$$

Where $\lambda = \begin{cases}0 & i\neq H_2O\\ 1 & i=H_2O\end{cases}$

A.1.2. Bubble Phase:

$$\begin{pmatrix}\text{Molar flow rate of } i \text{ assuming the entire bed is filled with bubbles}\end{pmatrix}\times\begin{pmatrix}\text{Fraction of the bed occupied by bubbles}\end{pmatrix} = \left(F_i^b\right)(\delta) \qquad \text{(A-13)}$$

$$\begin{pmatrix} Moles \\ in \end{pmatrix} - \begin{pmatrix} Moles \\ out \end{pmatrix} + \begin{pmatrix} Moles\ transported \\ to\ bubble\ surface \end{pmatrix} + \begin{pmatrix} Moles\ reacted\ in \\ bubble\ phase \end{pmatrix} = 0 \tag{A-14}$$

$$\begin{pmatrix} Moles \\ in \end{pmatrix} - \begin{pmatrix} Moles \\ out \end{pmatrix} = \left(F_i^b\big|_z - F_i^b\big|_{z+dz}\right) \times (\delta) \tag{A-15}$$

$$\begin{pmatrix} Moles\ transported \\ to\ bubble\ surface \end{pmatrix} = k_{be,i}\left(\frac{m}{s}\right).\Delta S_b\left(m^2\right).c_t\left(\frac{mole}{m^3}\right)\left(y_i^e - y_i^b\right) \tag{A-16}$$

$$\begin{bmatrix} Moles\ reacted\ in \\ bubble\ phase \end{bmatrix} = \gamma\left(\frac{m^3\ cat}{m^3\ bubble}\right) \times \Delta V_b\left(m^3\ bubble\right) \times \rho_p\left(\frac{kg\ cat}{m^3\ cat}\right).\sum_{m=1}^{n} \nu_{ij}\left(-r_{ij,b}\right)\left(\frac{mole}{kg\ cat.s}\right) \tag{A-17}$$

The steady-state mole balance then becomes

$$\delta\left(F_i^b\big|_z - F_i^b\big|_{z+dz}\right) + k_{be,i}\Delta S_b.c_t\left(y_i^e - y_i^b\right) + \gamma \times \Delta V_b \times \rho_p.\sum_{m=1}^{n} \nu_{ij}\left(-r_{ij,b}\right) = 0 \tag{A-18}$$

Dividing through by $\Delta V_t = A_c.\Delta z$ yields:

$$\frac{\delta\left(F_i^b\big|_z - F_i^b\big|_{z+dz}\right)}{A_c\Delta z} + k_{be,i}\frac{\Delta S_b}{\Delta V_t}.c_t\left(y_i^e - y_i^b\right) + \gamma \times \frac{\Delta V_b}{\Delta V_t} \times \rho_p.\sum_{m=1}^{n} \nu_{ij}\left(-r_{ij,b}\right) = 0 \tag{A-19}$$

where, ρ_p is the catalyst particle density (kg cat/m^3 cat), γ is the volume fraction of catalyst bed occupied by solid particles in bubble phase (m^3 cat /m^3 bubble), $r_{ij,b}$ is the reaction rate in bubble phase (mol/kg cat.s) and $\delta = \frac{\Delta V_b}{\Delta V_t}$ is the bubble phase volume as a fraction of total bed volume (m^3 bubble /m^3).

$$-\frac{\delta}{A_c}\frac{dF_i^b}{dz} + k_{be,i}.a_b.c_t\left(y_i^e - y_i^b\right) + \gamma \times \delta \times \rho_p.\sum_{m=1}^{n} \nu_{ij}\left(-r_{ij,b}\right) = 0 \tag{A-20}$$

A.1.3. Adsorbent Solid Phase:

$$\begin{pmatrix} Moles \\ in \end{pmatrix} - \begin{pmatrix} Moles \\ out \end{pmatrix} + \begin{pmatrix} Moles\ transported\ to \\ adsorbent\ solid\ surface \end{pmatrix} = 0 \tag{A-21}$$

$$\begin{pmatrix} Moles \\ in \end{pmatrix} - \begin{pmatrix} Moles \\ out \end{pmatrix} = \dot{m}_s\left(\frac{kg\ of\ adsorbent}{s}\right)q\left(\frac{mole}{kg\ of\ adsorbent}\right)\Bigg|_z - \dot{m}_s q\big|_{z+dz} \tag{A-22}$$

$$\begin{pmatrix} Moles\ transported\ to \\ adsorbentsolid\ \ surface \end{pmatrix} = k'_g \left(\frac{m}{s}\right) \times \Delta S_s \left(m^2\right) \times \left(q_e - q\right) \left(\frac{mole}{kg\ of\ adsorbent}\right) \times \rho_{ads} \left(\frac{kg\ of\ adsorbent}{m^3\ ads}\right) \times \beta \left(\frac{m^3\ ads}{m^3}\right) \quad \text{(A-23)}$$

Inserting Eqs. (A-22) and (A-23) into Eq. (A-21) yields:

$$\dot{m}_s q\big|_z - \dot{m}_s q\big|_{z+dz} + k'_g \times \Delta S_s \times \left(q_e - q\right) \times \rho'_s = 0 \quad \text{(A-24)}$$

Dividing by ΔV and considering the limit as ΔV → 0 yields:

$$\dot{m}_s \frac{q\big|_z - q\big|_{z+dz}}{A_c . \Delta z} + k'_g \times \frac{\Delta S_s}{\Delta V} \times \left(q_e - q\right) \times \rho'_s = 0 \quad \text{(A-25)}$$

By applying Eq. (A-10), (A-25) can be simplified into:

$$-\frac{\dot{m}_s}{A_c}\frac{dq}{dz} + k'_g \times a'_s \times \left(q_e - q\right) \times \rho'_s = 0 \quad \text{(A-26)}$$

$$\frac{\dot{m}_s}{A_c} = \rho'_s . u'_s \quad \text{(A-27)}$$

$$-\rho'_s . u'_s \frac{dq}{dz} + k'_g \times a'_s \times \left(q_e - q\right) \times \rho'_s = 0 \quad \text{(A-28)}$$

$$u'_s \frac{dq}{dz} = k'_g \times a'_s \times \left(q_e - q\right) \quad \text{(A-29)}$$

where, u'_s is the real flowing solids velocity ($m . s^{-1}$)

A.2. Energy Balance:

A.2.1. Emulsion and Bubble Phase:

$$\begin{pmatrix} Enthalpy \\ in \end{pmatrix} - \begin{pmatrix} Enthalpy \\ out \end{pmatrix} + \begin{pmatrix} Heat\ added\ \ from \\ emulsion\ phase \end{pmatrix} + \begin{pmatrix} Heat\ added\ \ from \\ bubble\ phase \end{pmatrix} + \begin{pmatrix} Heat\ added\ \ from \\ adsorbent\ surface \end{pmatrix} + \begin{pmatrix} Heat\ added\ \ from \\ surroundings \end{pmatrix} = 0 \quad \text{(A-30)}$$

$$\begin{pmatrix} Enthalpy \\ in \end{pmatrix} - \begin{pmatrix} Enthalpy \\ out \end{pmatrix} = \dot{m} \left(\frac{kg}{s}\right) c_p \left(\frac{J}{kg.K}\right) . T(K)\big|_z - \dot{m} c_p T\big|_{z+dz} \quad \text{(A-31)}$$

$$\left(\begin{matrix}Heat\ added\ from\\ emulsion\ phase\end{matrix}\right)=\Delta V_e\left(m^3\ emulsion\right)\times\rho_e\left(\frac{kg\,cat}{m^3\ emulsion}\right)\times\sum_{i=1}^{m}\left(\Delta H_i\right)\left(\frac{J}{mole}\right)\times\left(-r_i\right)\left(\frac{mole}{kg\,cat.s}\right) \tag{A-32}$$

$$\left(\begin{matrix}Heat\ added\ from\\ bubble\ phase\end{matrix}\right)=\Delta V_b\left(m^3\ bubble\right)\times\rho_p\left(\frac{kg\,cat}{m^3\ cat}\right)\times\gamma\left(\frac{m^3\ cat}{m^3\ bubble}\right)\times\sum_{i=1}^{m}\left(\Delta H_i\right)\left(\frac{J}{mole}\right)\times\left(-r_{i,b}\right)\left(\frac{mole}{kg\,cat.s}\right) \tag{A-33}$$

$$\left(\begin{matrix}Heat\ added\ from\\ adsorbent\ surface\end{matrix}\right)=h'_f\left(\frac{W}{m^2.K}\right)\Delta S_s\left(m^2\right).\left(T'_s-T\right)(K) \tag{A-34}$$

$$\left(\begin{matrix}Heat\ added\ from\\ surroundings\end{matrix}\right)=q_{conv}=U_i\left(\frac{W}{m^2.K}\right).A_s\left(m^2\right).\left(T^{shell}-T\right)(K) \tag{A-35}$$

By inserting Eqs. (A-31) - (A-35) into Eq. (A-30) and dividing by ΔV, the following is yield:

$$\frac{\dot{m}c_pT\big|_z-\dot{m}c_pT\big|_{z+dz}}{A_c.\Delta z}+\frac{\Delta V_e}{\Delta V_t}\rho_e\sum_{i=1}^{m}\left(\Delta H_i\right)\left(-r_i\right)+\gamma\frac{\Delta V_b}{\Delta V_t}\rho_p\sum_{i=1}^{m}\left(\Delta H_i\right)\left(-r_{i,b}\right)+h'_f\frac{\Delta S_s}{\Delta V_t}.\left(T'_s-T\right)+\frac{U.A_s}{\Delta V_t}.\left(T^{shell}-T\right)=0 \tag{A-36}$$

where, c_p is the specific heat capacity of the gaseous state at constant pressure (J/(kg·K)), T is the bulk gas-phase temperature (K), T^{shell} is the saturated water temperature (K), U is the overall heat transfer coefficient between the two sides (W/(m²·K)), h'_f is the gas–sorbent heat transfer coefficient(W/(m²·K)), and T'_s is the temperature of the flowing solid (K).

The area for heat transfer in the elemental volume is the circumference of the channel multiplied by length:

$$A_s=\pi D_i.dz \tag{A-37}$$

where, D_i is the tube internal diameter (m).

By considering the limit as ΔV → dV, we obtain the ordinary differential equation is obtained. Then Eqs. (A-10), (A-37), $\frac{\Delta V_e}{\Delta V_t}=(1-\delta)$ and $\frac{\Delta V_b}{\Delta V_t}=\delta$ in Eq. (A-36) are substituted with each other:

$$-\frac{1}{A_c}\frac{d\left(\dot{m}c_pT\right)}{.dz}+(1-\delta)\rho_e\sum_{i=1}^{m}\left(\Delta H_i\right)\left(-r_i\right)+\delta\gamma\rho_p\sum_{i=1}^{m}\left(\Delta H_i\right)\left(-r_{i,b}\right)+h'_f\,a'_s.\left(T'_s-T\right)+U\frac{\pi D_i.dz}{A_c.dz}.\left(T^{shell}-T\right)=0 \tag{A-38}$$

$$\dot{m}\left(\frac{kg}{s}\right)c_p\left(\frac{J}{kg.K}\right).T(K)=F_t\left(\frac{mole}{s}\right).C_p\left(\frac{J}{mole.K}\right).T(K) \tag{A-39}$$

Thus:

$$-\frac{1}{A_c}\frac{d\left(F_tC_pT\right)}{.dz}+(1-\delta)\rho_e\times\sum_{i=1}^{m}(\Delta H_i)(-r_i)+\delta\gamma\rho_p\times\sum_{i=1}^{m}(\Delta H_i)(-r_{i,b}) + h'_f\,a'_s.(T'_s-T)+U\frac{\pi D_i}{A_c}.(T^{shell}-T)=0 \tag{A-40}$$

Equation (A-40) is expressed as:

$$-\frac{C_{p,Mix}}{A_c}\frac{d(F_t.T)}{dz}+(1-\delta)\rho_e\times\sum_{i=1}^{m}(\Delta H_i)(-r_i)+\delta\gamma\rho_p\times\sum_{i=1}^{m}(\Delta H_i)(-r_{i,b}) + U\frac{\pi D_i}{A_c}.(T^{shell}-T)-h'_f\,a'_s.(T-T'_s)=0 \tag{A-41}$$

A.2.2. Adsorbent Solid Phase:

$$\begin{pmatrix}Entalpy\\in\\by\ solid\\mass\ flow\end{pmatrix}-\begin{pmatrix}Entalpy\\out\\by\ solid\\mass\ flow\end{pmatrix}-\begin{pmatrix}Rate\ of\ energy\\leaving\ the\ system\\by\ adsorbed\ mass\\of\ water\ flow\end{pmatrix}-\begin{pmatrix}Heat\ added\ from\\adsorbent\ surface\end{pmatrix}=0 \tag{A-42}$$

$$\begin{pmatrix}Rate\ of\ energy\\leaving\ the\ system\\by\ adsorbed\ mass\\of\ water\ flow\end{pmatrix}=\begin{pmatrix}Moles\ transported\ to\\adsorbent\ solid\ surface\end{pmatrix}\times\begin{pmatrix}Enthalpy\ of\\adsorption\end{pmatrix}_{H_2O} \tag{A-43}$$

$$=S'\left(\frac{kg\,ads}{m^2.s}\right)\times(q_e-q)\left(\frac{mole}{kg\,ads}\right)\times\Delta S_s\left(m^2\right)\times(\Delta H_{ads})_{H_2O}\left(\frac{J}{mole}\right)$$

$$\begin{pmatrix}Moles\ transported\ to\\adsorbent\ solid\ surface\end{pmatrix}=\begin{pmatrix}Molar\ flux\\of\ water\ adsorption\end{pmatrix}\times\begin{pmatrix}Surface\ area\\of\ water\ adsorbed\end{pmatrix}=$$

$$N_A.\Delta S_s=k'_g\left(\frac{m}{s}\right)\times(q_e-q)\left(\frac{mole}{kg\ of\ adsorbent}\right) \times\rho_{ads}\left(\frac{kg\ of\ ads}{m^3\ ads}\right)\times\beta\left(\frac{m^3\ ads}{m^3}\right)\times\Delta S_s\left(m^2\ ads\right) \tag{A-44}$$

$$\begin{pmatrix} Molar\ flux \\ of\ water\ adsorption \end{pmatrix} = \underbrace{k'_g\left(\frac{m}{s}\right)\times\rho_{ads}\left(\frac{kg\,ads}{m^3\,ads}\right)\times\beta\left(\frac{m^3\,ads}{m^3}\right)}_{S'\left(\frac{kg\,ads}{m^2.s}\right)}\times(q-q_e)\left(\frac{mol}{kg\,ads}\right) \tag{A-45}$$

$$\begin{pmatrix} Mass\ flux \\ of\ water\ adsorption \end{pmatrix} = S'\left(\frac{kg\,ads}{m^2.s}\right) = k'_g\left(\frac{m}{s}\right)\times\rho'_s\left(\frac{kg\,ads}{m^3}\right) \tag{A-46}$$

$$\begin{pmatrix} Entalpy \\ in \\ by\,solid \\ mass\,flow \end{pmatrix} - \begin{pmatrix} Entalpy \\ out \\ by\,solid \\ mass\,flow \end{pmatrix} = \dot{m}_s c'_{ps}\times T'_s(K)\big|_z - \dot{m}_s c'_{ps} T'_s\big|_{z+dz} \tag{A-47}$$

$$\begin{pmatrix} Heat\,added\ from \\ adsorbent\,surface \end{pmatrix} = h'_f\left(\frac{W}{m^2K}\right).\Delta S_s(m^2).(T_s'-T)(K) \tag{A-48}$$

where, c'_{ps} is the specific heat of the flowing solid at constant pressure (J kg^{-1} K^{-1}) , ΔH_{ads} is the specific heat of adsorption (J mol^{-1}), $\dot{m}_s$ is the mass flow rate of adsorbent solid particle (kg s^{-1}) and S' is the mass flux of water adsorption (kg m^{-2} s^{-1}).

At this stage, Eqs. (A-43), (A-47) and (A-48) into Eq. (A-42) are substituted with each other to yield an expression for the energy balance in adsorbent solid particle:

$$\dot{m}_s c'_{ps} T_s'(K)\big|_z - \dot{m}c_p T_s'\big|_{z+dz} - h'_f.\Delta S_s.(T'_s-T) + S'.\Delta S_s.(q_e-q)\times(-\Delta H_{ads}) = 0 \tag{A-49}$$

Dividing by $\Delta V = A_c.\,\Delta z$ and taking the limit as $\Delta z \to 0$:

$$\frac{\dot{m}_s c'_{ps} T_s'(K)\big|_z - \dot{m}_s c'_{ps} T_s'\big|_{z+dz}}{A_c\Delta z} - h'_f.\frac{\Delta S_s}{\Delta V}.(T_s'-T) + S'.\frac{\Delta S_s}{\Delta V}.(q_e-q)\times(-\Delta H_{ads}) = 0 \tag{A-50}$$

$$-\frac{\dot{m}_s c'_{ps}}{A_c}\frac{dT_s'}{dz} - h'_f.a'_s.(T_s'-T) + S'.\frac{\Delta S_s}{\Delta V}.(q_e-q)\times(-\Delta H_{ads}) = 0 \tag{A-51}$$

Substituting $\frac{\dot{m}_s}{A_c} = \rho'_s.u_s$ with $a'_s = \frac{\Delta S_s}{\Delta V}$ in Eq. (A-51) the following is yield:

$$\rho'_s.u_s.c'_{ps}\frac{dT'_s}{dz} = -h'_f.a'_s.(T'_s-T) + S'.a'_s.(q_e-q)\times(-\Delta H_{ads}) \tag{A-52}$$

$$u_s.\rho'_s.c'_{ps}\frac{dT'_s}{dz} = (-\Delta H_{ads})S'.a'_s.(q_e-q) + h'_f.a'_s.(T-T'_s) \tag{A-53}$$

Appendix B: Nomenclature

a_b	Bubble surface area, $m^2\ m^{-3}$
A_c	Tube cross section area, m^2
a'_s	Adsorbent solid surface area, $m^2\ m^{-3}$
Cp_g	Specific heat of the gas at constant pressure, J $mol^{-1}\ K^{-1}$
c_p	Specific heat of the gas at constant pressure, J $kg^{-1}\ K^{-1}$
Cp'_s	Specific heat of the adsorbent solid at constant pressure, J $kg^{-1}\ K^{-1}$
C_t	Total concentration, mol m^{-3}
D	Reactor diameter, m
d_b	Bubble diameter, m
D_i	Diameter of inside tube, m
D_o	Diameter of outside tube, m
d_c	Diameter of catalyst, m
d_s	Diameter of adsorbent solid, m
F_i	Molar flow of species i, mole s^{-1}
F^e	Molar flow in emulsion side, mole.s^{-1}
F^b	Molar flow in bubble side, mole.s^{-1}
$\Delta H_{f,i}$	Enthalpy of formation of component i, J mol^{-1}
h'_f	Gas-solid heat transfer coefficient, W $m^{-2}\ K^{-1}$
h_i	Heat transfer coefficient between fluid phase and reactor wall, W $m^{-2}\ K^{-1}$
h_o	Heat transfer coefficient between coolant stream and reactor wall, W $m^{-2}\ K^{-1}$
K_{bei}	Mass transfer coefficient for component i in fluidized-bed, m.s^{-1}
k'_g	Gas-solid mass transfer coefficient, m s^{-1}
L	Length of reactor, m
P_t	Total pressure, bar
q	Concentration of water adsorbed in flowing solids, mol kg^{-1}
q_e	Equilibrium concentration of adsorbed water, mol kg^{-1}
R	Universal gas constant, J $mol^{-1}\ K^{-1}$
r_i	Reaction rate of component i, mol $kg^{-1}\ s^{-1}$
r_{bi}	Reaction rate of component i in bubble phase, mol.kg^{-1}.s^{-1}
S'	Mass flux of water adsorption, kg $m^{-2}\ s^{-1}$
T_g	Bulk gas phase temperature, K
T_s	Temperature of catalyst phase, K
T'_s	Temperature of flowing solids, K
T_{shell}	Temperature of coolant stream, K
W	water content
U_i	Overall heat transfer coefficient between coolant and process streams, W $m^{-2}\ K^{-1}$
u_b	Velocity of rise of bubbles, m.s^{-1}
u_g	Superficial gas velocity, m s^{-1}
u_{mf}	Velocity at minimum fluidization, m s^{-1}
u'_s	Real flowing solids velocity, m s^{-1}
y_i	Mole fraction of component i in the fluid phase, mol mol^{-1}
y_i^b	Mole fraction of component i in the bubble phase
y_i^e	Mole fraction of component i in the emulsion phase
z	Axial reactor coordinate, m
Z	Compressibility factor

Greek letter

ε_{mf}	Void fraction of catalytic bed at minimum fluidization
ß	Solid holdup
ρ	Density of fluid phase, kg m^{-3}
ρ_B	Density of catalytic bed, kg m^{-3}
ρ_e	Emulsion phase density, kg m^{-3}
ρ_p	Particle density, kg m^{-3}
ρ_{ads}	Adsorbent density, kg m^{-3}
δ	Bubble phase volume as a fraction of total bed volume
η	Effectiveness factor
β	flowing solid holdup
μ	Dynamic viscosity, Pa s
ρ'_S	Flowing solid density, kg m^{-3}
γ	Volume fraction of catalyst occupied by solid particle in bubble

Abbreviations

SE-FMR	Sorption enhanced fluidized-bed methanol reactor
FMR	Fluidized-bed methanol reactor

CMR Conventional methanol reactor

References

Bayat, M., Dehghani, Z., Hamidi, M., Rahimpour, M.R., 2014a. Methanol synthesis via sorption-enhanced reaction process: Modeling and multi-objective optimization. J. Taiwan Inst. Chem. Eng. 45, 481-494.

Bayat, M., Dehghani, Z., Rahimpour, M.R., 2014b. Dynamic multi-objective optimization of industrial radial-flow fixed-bed reactor of heavy paraffin dehydrogenation in LAB plant using NSGA-II method. Journal of the Taiwan Institute of Chemical Engineers 45, 1474-1484.

Bayat, M., Dehghani, Z., Rahimpour, M.R., 2014c. Sorption-enhanced methanol synthesis in a dual-bed reactor: Dynamic modeling and simulation. J. Taiwan Inst. Chem. Eng. 45, 2307-2318.

Bayat, M., Hamidi, M., Dehghani, Z., Rahimpour, M.R., 2014d. Sorption-enhanced Fischer–Tropsch synthesis with continuous adsorbent regeneration in GTL technology: Modeling and optimization. J. Ind. Eng. Chem. 20, 858-869.

Bayat, M., Hamidi, M., Dehghani, Z., Rahimpour, M.R., Shariati, A., 2013. Sorption-enhanced reaction process in Fischer–Tropsch synthesis for production of gasoline and hydrogen: Mathematical modeling. J. Nat. Gas Sci. Eng 14, 225-237.

Bayat, M., Hamidi, M., Dehghani, Z., Rahimpour, M.R., Shariati, A., 2014e. Hydrogen/methanol production in a novel multifunctional reactor with in situ adsorption: modeling and optimization. Int. J. Energy Res. 38, 978-994.

Bayat, M., Rahimpour, M.R., Taheri, M., Pashaei, M., Sharifzadeh, S., 2012. A comparative study of two different configurations for exothermic–endothermic heat exchanger reactor. Chemical Engineering and Processing: Process Intensification 52, 63-73.

Davidson, J.F., Harrison, D., 1963. Fluidized Particles. Cambridge University Press, New York.

Dehghani, Z., Bayat, M., Rahimpour, M.R., 2014. Sorption-enhanced methanol synthesis: Dynamic modeling and optimization. J. Taiwan Inst. Chem. Eng. 45, 1490-1500.

Deshmukh, S.A.R.K., Laverman, J.A., Cents, A.H.G., van Sint Annaland, M., Kuipers, J.A.M., 2005. Development of a Membrane-Assisted Fluidized Bed Reactor. 1. Gas Phase Back-Mixing and Bubble-to-Emulsion Phase Mass Transfer Using Tracer Injection and Ultrasound Experiments. Industrial and Engineering Chemistry Research 44, 5955-5965.

Everett, G., Retallick, W.B., 1963. Method for the production of hydrogen. Google Patents.

Goossens, W.R.A., Dumont, G.L., Spaepen, G.L., 1971. Fluidization of binary mixtures in the laminar flow region, Chemical Engineering Progress Symposium Series, pp. 38-45.

Graaf, G.H., Scholtens, H., Stamhuis, E.J., Beenackers, A.A.C.M., 1990. Intra-particle diffusion limitations in low-pressure methanol synthesis. Chemical Engineering Science 45, 773-783.

Holman, J.P., 1989. Heat transfer. McGraw-Hill, New York: .

Johnsen, K., Ryu, H.J., Grace, J.R., Lim, C.J., 2006. Sorption-enhanced steam reforming of methane in a fluidized bed reactor with dolomite as -acceptor. Chemical Engineering Science 61, 1195-1202.

Kunii, D., Levenspiel, O., 1991. Fluidization engineering. Wiley, New York.

Mori, S., Wen, C.Y., 1975. Estimation of bubble diameter in gaseous fluidized beds. AIChE J. 21, 109-115.

Peng, D.-Y., Robinson, D.B., 1976. A New Two-Constant Equation of State. Industrial and Engineering Chemistry Fundamentals 15, 59-64.

Perry, R.H., Green, D.W., Maloney, J.O., 1977. Perry's Chemical Engineers' Handbook, 7th ed. ed. McGraw-Hill.

Rahimpour, M.R., Bayat, M., Rahmani, F., 2010. Enhancement of methanol production in a novel cascading fluidized-bed hydrogen permselective membrane methanol reactor. Chemical Engineering Journal 157, 520-529.

Rahimpour, M.R., Elekaei, H., 2009. Enhancement of methanol production in a novel fluidized-bed hydrogen-permselective membrane reactor in the presence of catalyst deactivation. International Journal of Hydrogen Energy 34, 2208-2223.

Rahimpour, M.R., Lotfinejad, M., 2008. A comparison of co-current and counter-current modes of operation for a dual-type industrial methanol reactor. Chemical Engineering and Processing 47, 1819-1830.

Schack, C.J., McNeil, M.A., Rinker, R.G., 1989. Methanol synthesis from hydrogen, carbon monoxide, and carbon dioxide over a CuO/ZnO/Al2O3 catalyst: I. Steady-state kinetics experiments. Appl. Catal. 50, 247-263.

Tatlıer, M., Erdem-Şenatalar, A., 2000. Optimization of the cycle durations of adsorption heat pumps employing zeolite coatings synthesized on metal supports. Microporous and Mesoporous Materials 34, 23-30.

Vakili, R., Setoodeh, P., Pourazadi, E., Iranshahi, D., Rahimpour, M.R., 2011. Utilizing differential evolution (DE) technique to optimize operating conditions of an integrated thermally coupled direct DME synthesis reactor. Chemical Engineering Journal 168, 321-332.

Wagialla, K.M., Elnashaie, S.S.E.H., 1991. Fluidized-bed reactor for methanol synthesis. A theoretical investigation. Industrial and Engineering Chemistry Research 30, 2298-2308.

Zhu, W., Gora, L., van den Berg, A.W.C., Kapteijn, F., Jansen, J.C., Moulijn, J.A., 2005. Water vapour separation from permanent gases by a zeolite-4A membrane. Journal of Membrance Science 253, 57-66.